Published in final edited form as:
Mol Cancer Res. 2011 December ; 9(12): 1668–1685. doi:10.1158/1541-7786.MCR-10-0563.

Autocrine endothelin-3/endothelin receptor B signaling maintains cellular and molecular properties of glioblastoma stem cells

Yue Liu[1], **Fei Ye**[1,2], **Kazunari Yamada**[1], **Jonathan L. Tso**[1], **Yibei Zhang**[1], **David H. Nguyen**[1], **Qinghua Dong**[1,3], **Horacio Soto**[4], **Jinny Choe**[1], **Anna Dembo**[1], **Hayley Wheeler**[1], **Ascia Eskin**[5], **Ingrid Schmid**[6], **William H. Yong**[7,10], **Paul S. Mischel**[7,10], **Timothy F. Cloughesy**[8,10], **Harley I. Kornblum**[9,10], **Stanley F. Nelson**[5,10], **Linda M. Liau**[4,10], and **Cho-Lea Tso**[1,10]

[1]Department of Surgery/Surgical Oncology, David Geffen School of Medicine, University of California Los Angeles, Los Angeles, California

[2]Department of Neurosurgery, Tongji Hospital, Tongji Medical College, Huazhong University of Science and Technology, Wuhan, Hubei, P. R. China

[3]Cancer Institute, Zhejiang University, Hangzhou, Zhejiang, P. R. China

[4]Department of Neurosurgery, David Geffen School of Medicine, University of California Los Angeles, Los Angeles, California

[5]Department of Human Genetics, David Geffen School of Medicine, University of California Los Angeles, Los Angeles, California

[6]Department of Medicine/Hematology-Oncology, David Geffen School of Medicine, University of California Los Angeles, Los Angeles, California

[7]Department of Pathology and Laboratory Medicine, David Geffen School of Medicine, University of California Los Angeles, Los Angeles, California

[8]Department of Neurology, David Geffen School of Medicine, University of California Los Angeles, Los Angeles, California

[9]Department of Psychiatry, David Geffen School of Medicine, University of California Los Angeles, Los Angeles, California

[10]Jonsson Comprehensive Cancer Center, University of California Los Angeles, Los Angeles, California

Abstract

Glioblastoma stem cells (GSC) express both radial glial cell (RGC) and neural crest cell (NCC)-associated genes. We report that endothelin 3 (EDN3), an essential mitogen for NCC development and migration, is highly produced by GSC. Serum-induced proliferative differentiation rapidly decreased EDN3 production and downregulated the expression of stemness-associated genes, and reciprocally, two glioblastoma markers, EDN1 and YKL-40 transcripts, were induced. Correspondingly, patient glioblastoma tissues express low levels of EDN3 mRNA and high levels of EDN1 and YKL-40 mRNA. Blocking EDN3/endothelin receptor B (EDNRB) signaling by an EDNRB antagonist (BQ788), or EDN3 RNA interference (siRNA), leads to cell apoptosis and functional impairment of tumor-sphere formation and cell spreading/migration in culture, and loss

Correspondence should be addressed to: Cho-Lea Tso, Ph.D., Factor Building, Rm 13-260, 10833 Le Conte Avenue, Department of Surgery/Surgical Oncology, David Geffen School of Medicine at UCLA, Los Angeles, CA 90095, ctso@mednet.ucla.edu, Phone: 310-825-1066.

of tumorigenic capacity in animals. Using exogenous EDN3 as the sole mitogen in culture does not support GSC propagation, but can rescue GSC from undergoing cell apoptosis. Molecular analysis by gene expression profiling revealed that most genes downregulated by EDN3/EDNRB blockade were those involved in cytoskeleton organization, pause of growth and differentiation, and DNA damage response, implicating the involvement of EDN3/EDNRB signaling in maintaining GSC migration, undifferentiation, and survival. These data suggest that autocrine EDN3/EDNRB signaling is essential for maintaining GSC. Incorporating END3/EDNRB-targeted therapies into conventional cancer treatments may have clinical implication for the prevention of tumor recurrence.

Keywords

Glioblastoma; cancer stem cells; endothelin 3; radial glial cells; neural crest cells; neural stem cells

Introduction

Glioblastoma, (WHO grade IV) is the most common and most aggressive type of primary brain tumor in humans. It remains virtually incurable despite extensive surgical excision and post-operative adjuvant radiotherapy and chemotherapy (1). Glioblastoma stem cells (GSC) have been recently isolated from patients' glioblastoma tumors and were characterized as a small subset of stem-like tumor cells capable of initiating and sustaining tumor growth when grafted into mice (2–6). Although CD133/prominin, a normal neural stem cell (NSC) marker, is not an obligatory marker for GSC (6, 7), CD133 was first applied as a surface marker for isolation and enrichment of GSC (2–5, 7–9). Tumors initiated from CD133+ GSC often recapitulate the histopathological features of the patient tumors from which the cells were derived, indicating the ability to self-renew and reproduce the cellular heterogeneity found in human glioblastoma tumors (2, 4–6). Studies showed that CD133+ tumor-initiating cells possess marked resistance to radio-chemotherapy (10, 11), and thus are now suggested to be responsible for post-treatment failure and tumor recurrence.

The molecular profiles of GSC revealed characteristics of neuroectodermal-like cells, expressing both neural and mesenchymal developmental genes, and portraying an undifferentiated, migratory, astrogliogenic, and chondrogenic phenotype (8). This suggests that a subset of GSC may inherit NCC-like developmental pathways to initiate a tumor. In particular, endothelin 3 (EDN3), a potent mitogen for NCC and its derived lineage precursor cells (12, 13), was identified as one of the top genes highly expressed in tumorigenic GSC (8). EDN3 is a member of the endothelin (EDN) family, which consists of a group of vasoactive peptides referred to as EDN1, EDN2, and EDN3 (14). EDNs are synthesized initially as inactive larger precursor molecules and then post-translationally cleaved by endothelin-converting enzyme (ECE-1) to yield the biologically active 21-amino acid form (15). The effects of EDNs are mediated by two distinct but highly homologous G-protein-coupled receptors, EDN receptor A (EDNRA) and EDN receptor B (EDNRB), in an autocrine and paracrine manner (16, 17). The EDNRA predominantly binds to EDN1 and EDN2 with similar affinities, and EDN3 with 1000–2000-fold lower affinity, whereas EDNRB has similar affinities for all three isopeptides (18). Mutations in EDN3 or EDNRB can lead to abnormal development of the enteric nervous system (ENS) and melanocytes and are known to account for the majority of patients with Waardenburg syndrome (WS) type IV, who exhibit both pigmentation and megacolon phenotypes (19, 20). EDN3 and EDNRB mRNA expression has been reported in fetal human enteric mesenchyme and neural crest cells (21), and EDN3/EDNRB signaling is known to influence NCC proliferation, differentiation, and migration during ENS development (22). The expression of the EDN

system genes has been demonstrated in the brain and in human glioblastoma (23, 24) as well as a broad range of other types of human cancers (25). The role of the EDN-axis, especially in EDN1-axis, has been implicated in promoting tumor progression. Blocking EDN receptors has been suggested as a novel strategy in cancer therapy (25).

In this study, we provide the first comprehensive analysis of the expression and function of the endothelin system in patient-derived GSC. We found an essential role of autocrine EDN3/EDNRB system in GSC. Blocking either EDNRB function or EDN3 production leads to GSC apoptosis and loss of migration, self-renewal and tumorigenesis. Furthermore, genome-wide expression array analysis have elucidated molecular pathways and gene-network connections to this essential signaling for maintaining GSC. This finding implicates that the EDN3/EDNRB signaling pathway may serve a novel therapeutic target for the development of potentially more effective treatment protocols for preventing GSC-mediated tumor recurrence.

Materials and Methods

Glioblastoma sphere culture

Glioblastoma tumor specimens were obtained from patients who underwent surgery at Ronald Reagan UCLA Medical Center. All samples were collected under protocols approved by the UCLA Institutional Review Board. Dissociated tumor cells from fresh tumor tissue were cultured in a serum-free media containing DMEM/Ham's F-12 (Mediatech) supplemented with 20 ng/ml human recombinant epidermal growth factor (EGF, Sigma), 20 ng/ml basic fibroblast growth factor (FGF, Millipore), 10 ng/ml leukemia inhibitory factor (LIF, Millipore), and 1x B27 without vitamin A (Invitrogen), and is designated as stem cell growth factor (SGF) media. The tumorigenicity of GSC was verified in xenograft animals (8). In parallel, autologous glioblastoma cell lines were established by propagating cells in DMEM/Ham's F-12 media supplemented with 10% fetal bovine serum.

Fluorescence-activated cell sorting analyses (FACS) and purification of CD133+ GSC

$2–5 \times 10^5$ dissociated cells from glioblastoma tumor sphere cultures were stained with anti-CD133-APC (Miltenyi Biotech) for 20 minutes at 4°C. The analyses for CD133 positive cells were performed on a FACSCalibur flow cytometer (Becton Dickinson) and ≥ 10,000 events were collected in each analysis. To purify CD133+ cells, dissociated glioblastoms sphere cultures or enzyme digested tumor xenografts were immunostained with anti-CD133 APC under sterile conditions. The CD133+ and CD133− cells were sorted and collected on a BD FACSAria™ II cell sorter at 70 psi using a 70-μm nozzle.

Quantitative (qt) reverse transcriptase polymerase chain Reaction (RT-PCR) analysis

Total RNA was extracted using a RNeasy kit (QIAGEN). Two micrograms of RNA from each sample were transcribed to cDNA using a Taqman RT Reagent Kit (Applied Biosystems). PCR was performed, using 5 μl cDNA equivalents to 100 ng total RNA and was carried out by using SYBR Green PCR Core Reagents (Applied Biosystems). After amplification, PCR products (5 μl) were electrophoresed on 2% agarose gel. The primer sequences and expected size of amplified PCR products are described in Supplemental Information.

Immunocytochemical, histopathological, and immunohistochemical analysis

GSC were fixed in 4% parafomaldehyde and then singly or doubly stained with anti-CD133 (1:100, Abcam), anti-nestin (1:200, Chemicon) or anti-EDN3 (1:200, Santa Cruz Biotech) antibodies. After washing, cells were incubated with rhodamine red-conjugated anti-mouse or Alexa Fluor 488–conjugated anti-rabibit antibodies (Invitrogen). Nuclei were

counterstained with Hoechst 33342 (Invitrogen). Histopathological analyses were performed on frozen section or paraffin slides stained with Hematoxylin and Eosin (H–E) staining as per standard technique. Immunohistochemical staining was performed on paraffin slides. Slides were subject to a 1-h blocking step followed by the application of primary antibody or control antibody for 1 h at room temperature. The following primary antibodies were used: CD133 (1:100, Abcam), EDN3 (1:100, Epitomics), EDN1 (1:250, Abcam), EDNRB (1:100, Epitomics), and EDNRA (1:200, ENZO life Science). The immunodetection was performed using Vectastain ABC Standard kit and Vector NovaRED (Vector Laboratories).

Enzyme-linked immunosorbent assay (ELISA)

To determine the amount of EDN3 released from GSC, dissociated GSC were plated in 24-well plates in triplicate at the density of 5×10^4 cells per ml per well. Four hours later, stem cell culture media was replaced with fresh SGF media with or without ECE-1 inhibitor, plain media or serum-containing media. The respective conditioned media was collected at various time points and were stored at −80°C. The amount of EDN3 peptides in condition media was determined by an ELISA kit specific for EDN3 (Immuno-Biological Laboratories). The absorbance was read at 450 nm by Epoch Microplate Reader (BioTek Instruments).

Flow cytometric analysis for cell cycle distribution and cell apoptosis

To determine the effects of BQ788, BQ123, or combination treatment on cell cycle distribution and cell apoptosis, $2–5 \times 10^5$ treated and untreated GSC were stained with propidium iodide (PI)-based hypotonic DNA staining buffer. Cell cycle distribution for ~10,000 cells was analyzed using a FACScan (Becton Dickinson). Apoptotic cells with degraded DNA were detected as a hypodiploid or ‘sub-G1’ peak in a DNA histogram.

Proliferation assay for GSC

The effects of BQ788 and/or BQ123 treatment on the proliferative activity of GSC were determined by a 3-(4,5-dimethylthiazol-2-yl)-5-(3-carboxymethoxyphenyl)-2-(4-sulfophenyl)-2H-tetrazolium (MTS/PMS) colorimetric assay according to the manufacturer’s instructions (Promega). Cells were seeded into 96-well tissue culture plates at a density of 2,000 cells per well in the presence or absence of EDNRA or EDNRB antagonists and incubated for 72 hours. The absorbance was measured at 490 nm after a 4-hour incubation with MTS/PMS reagents.

Quantitative measurement of cell apoptosis and cell viability

To determine whether EDN3 alone can support GSC survival, cell apoptosis assays were performed by using a Cell Death Detection ELISAPLUS kits (Roche), which quantitatively detects the amount of cleaved DNA/histone complexes (nucleosomes) in a given sample. The GSC were seeded at the concentration of 2000 cells/well/100 μl in triplicates. The culture media was changed and switched to plain media that contain various concentrations of EDN3. Cell apoptosis was measured after 72 hr incubation by reading the absorbance at 405 nm. The same method was applied to the measurement of BQ788 and EDN3siRNA treatment-induced cell apoptosis. The viability of GSC was determined by Trypan Blue staining (Invitrogen).

Knockdown of EDN3 by siRNA transfection

A reverse transfection protocol was performed to deliver EDN3 siRNA (Ambion), non-silencing control siRNA (Ambion) or GAPDH siRNA (Dharmacon) into GSC. Briefly, a transfection complex was prepared by diluting siRNA in 10 μL OPTI-MEMI (Invitrogen) then adding 10 μL OPTI-MEMI containing 0.3 μL Lipofectamine RNAiMAX transfection

reagent (Invitrogen). This complex was then added into each well in 96-well plate followed by seeding 6000 GSC in 100 ul SGF media to give a final siRNA concentration of 30 nM in each well. EDN3 gene silencing was determined 72 hrs after transfection by qtRT-PCR, using Power SYBR® Green Cells-to-CT™ Kit (Ambion).

Intracranial tumor formation assay and histopathological analysis

The role of EDN3/EDNRB signaling in maintaining the tumorigenic capacity of GSC was examined in Beige/SCID mice. 10^4 live GSC cells treated with and without 50 μM BQ788 for 24 hrs were injected in a total volume of 3μl into brains of mice under a UCLA Institutional Animal Research Committee–approved protocol. Mice were maintained for 25 weeks or until development of neurological signs. Brains of euthanized mice were collected, fixed in 10% formalin, paraffin-embedded, and sectioned. Alternatively, brain tissue was placed in O.C.T. embedding medium (Tissue-Tekm), dipped in liquid nitrogen, and sectioned in a −20°C cryostat. Histopathological analyses were performed on frozen section or paraffin slides stained with H-E stainingas per standard technique.

Microarray procedures, data analysis and gene annotation

Molecular profiling of 6 untreated (n=3, duplicate) and 3 BQ788 treated GSC (n=3) were performed using standard Affymetrix protocols and hybridized to Affymetrix GeneChip U133 Plus 2.0 Array as described previously (8). The DCP files were globally normalized, and gene expression values were generated using the dChip implementation of perfect-match minus mismatch model-based expression index. The group comparisons were performed in dChip and samples were permuted to assess the false discovery rate (FDR). To avoid inclusion of low level and unreliable signals the difference of the means needed to exceed 100 and be called present by MAS 5.0 in greater than 20% of the samples. In addition, the Gene Set Enrichment Analysis (GSEA) tool was performed to identify significant gene ontology groups that were enriched (26). Functional annotation of individual gene was obtained from NCBI/Entrez Gene (http://www.ncbi.nlm.nih.gov/sites/entrez), UniProt (http://www.uniprot.org/), information hyperlinked over protein (http://www.ihop-net.org/) and the published literature in PubMed Central (http://www.ncbi.nlm.nih.gov/pubmed).

Statistical analysis

Each experiment was set up in triplicate and repeated at least twice. Data were expressed as means ± SD and analyzed using one-way ANOVA tests, depending on homogeneity of variances. All *P*-values were two-sided, and values less than 0.05 were considered significant. SPSS v13.0 for Windows software was used for all statistical analysis.

Results

Expression of the endothelin system components in GSCs

Through genome-wide expression microarray analysis, we previously identified EDN3 as one of the most overexpressed transcripts in tumorigenic GSC when compared to autologous, differentiated glioblastoma cells cultured in serum-containing media (8). We thus hypothesized that EDN3 may contribute to maintaining GSC properties. To test this hypothesis, we first investigated the expression of the EDN system genes in GSC cultures. Three patient-derived tumorigenic GSC lines (D431, S496, and E445), which contain 39.6%, 9.6%, and 1.5 % CD133+ cells, respectively, were employed for this study (Figure 1A). GSC, which form semi-adherent tumor spheres with highly-motile cells, spontaneously migrate outward from sphere bodies (Figure 1A). We tested both unsorted and sorted CD133+ and CD133− cells from D431 and S496 GSC cultures, as well as the autologous

CD133− glioblastoma cell lines passaged in serum-containing media. Since E445 GSC cultures contain only 1.5% CD133+ cells, we only tested the unsorted cell population. By using qtRT-PCR analysis, mRNA expression of EDN-1, EDNRA, EDNRB, and ECE-1 was detected in all glioblastoma cell samples tested. Notably, the expressions level of EDN1 and EDNRA mRNAs were particularly upregulated in all glioblastoma cell lines cultured in 10% serum, while high levels of EDN3 mRNA was only detected in GSC lines established in SGF media, unsorted GSC, or sorted CD133+ or CD133-cells (Figure 1B). EDN3 mRNA appears to not be a SGF responsive gene or direct target of SGF, since switching serum-cultured glioblastoma cells to SGF for 6, 24, and 48 hrs (Figure 1B, not shown) did not stimulate comparable EDN3 mRNA expression in glioblastoma cells (Figure 1B). This data indicates that EDN3, but not EDN1, is a molecular/cellular signature for GSCs. Although both CD133+ and CD133− cells sorted from glioblastoma sphere cultures express EDN3, differentiated CD133− glioblastoma cell lines cultured in serum do not express EDN3, indicating that EDN3 is only expressed in GSC and its immediately differentiated CD133- daughter cells maintained in stem cell culture condition. The data also suggest that GSC lines represent different cell populations from autologous glioblastoma cell lines, which cannot be subsequently reversed following transition to SGF conditions (27)

Upregulation of EDN3 mRNA coupled with downregulation of EDN1 mRNA expression characterizes stemness state of GSCs

EDN1 has been implicated in the growth and progression of a wide range of human tumors (25); while recently, EDN3 has been suggested as a tumor suppressor gene in female malignances (28, 29). Since we detected a reciprocal relationship in the expression of EDN1 and EDN3 mRNA in glioblastoma cells cultured under different conditions, we examined whether there is a reciprocal regulation of EDN1 and EDN3 in GSC. Fetal bovine serum (FBS), which contains a variety of cytokines and growth factors, was used as a surrogate for inflammatory mediators to force GSC cultures to undergo proliferative differentiation as transit-amplifying-like cells capable of proliferation and differentiation, which eventually can be propagated as glioblastoma cell lines (Figure 2A). Progressively diminished EDN3 mRNA expression coupled with marked induction of EDN1 mRNA was seen in serum-stimulated GSC cultures (Figure 2B). Serum-induced GSC differentiation was further characterized by the co-downregulation of several RGC- and NSC-associated genes expressed by GSC (8) (Figure 2B), including fatty acid-binding protein 7 (FABP7) (30), CD133 (31), sex-determining region Y-box 2 (SOX2) (32), inhibitor of DNA binding 4 (ID4) (33) and GAP43 (34), suggesting that EDN3 is a marker for undifferentiated, stem-like glioblastoma cells. In contrast, the expressions of EDN1 (glioblastoma tumor marker) (23) and YKL-40 mRNA (glioblastoma prognostic marker; (35); only expressed in D431 and S496), were induced as a result of proliferative differentiation (Figure 2B). The mRNA level of topoisomerase (DNA) II alpha (TOP2A), a maker that is associated with cell growth, was unchanged. This data supports the notion that the reciprocal regulation of EDN3 and EDN1 expression in GSC may modulate and determine tumor development (36, 37). Indeed, the transcripts of EDN system genes were determined in patient-derived glioblastoma tumors, and elevated expression of EDN1 mRNA was determined in all 11 tumors analyzed, whereas EDN3 mRNA was expressed at a lower level in the majority of tested primary tumors when compared to EDN1 mRNA (Figure 2C). Likewise, YKL-40 mRNA was expressed in most glioblastoma tumors (Figure 2C).

GSCs are actively secreting EDN3 peptides when maintained in SGF conditions

Since EDN3 mRNA is uniquely expressed in GSC, but not in more differentiated autologous glioblastoma cells cultured in the serum, we then tested whether EDN3 was expressed at the protein level and secreted by GSC maintained in SGF media. Immunostaining analysis revealed that EDN3 was only expressed in GSC, but not in autologous glioblastoma cells

cultured in serum-containing media (Figure 3A). Moreover, sorted CD133+ GSC co-expressed EDN3 and CD133 or nestin, whereas glioblastoma cell lines only expressed nestin, not EDN3 or CD133. Either CD133+ or CD133− cells in all three tested sphere cultures express EDN3 as determined by two-color flow cytometric analysis (Supplementary Figure 1). ELISA assays further confirmed that the conditioned media collected from GSC cultures contained high concentration of EDN3, while no EDN3 peptides were measured in conditioned media collected from glioblastoma cell line cultures (Figure 3B). The production of EDN3 peptides by GSC cultures was markedly decreased when cultures were switched to plain media or serum-containing media (1 week), or treated with the ECE-1 inhibitor SM-19721, by which GSC were forced to undergo starvation, proliferative differentiation and acute EDN3 deficiency (Figure 3B). These data confirmed that bioactive EDN3 peptides were only actively secreted by GSC maintained in SGF media. Moreover, under light microscope, acute cell death was observed when GSC were treated with the ECE-1 inhibitor (Figure 3C), suggesting that autocrine EDN3 may be an essential survival factor only when GSC are maintained in SGF conditions, not when GSC undergo cell differentiation.

Blockade of EDNRB, not EDNRA, signaling induces GSC apoptosis without prominent cell cycle arrest

Since proteolytic processing of endothelin precursors to biologically active peptides by ECE-1 is not specific to EDN3, we then analyzed and compared the effects of EDNRB and EDNRA antagonists on GSC. GSC were treated for 72 hrs with various doses of the EDNRB antagonist BQ788 or the EDNRA antagonist BQ123. Evidently, structural/morphological alterations and cell apoptosis were only detected in GSC treated with BQ788, not BQ123 or vehicle control (ethanol), as examined microscopically, and BQ788-induced morphological changes and cell apoptosis were significantly enhanced in a dose-dependent manner (Figure 4A). Correspondingly, the increase in apoptotic cells (2.5–4 fold) appeared in a sub-G1 peak in DNA histograms analyzed by flow cytometric analysis and was only found in GSC treated with BQ788 (50 μM), not BQ123 (50 μM), in all three GSC cultures tested (Figure 4B). Notably, no major changes were found in the cell cycle distribution in BQ788-treated GSC when compared to untreated control cells. Only slightly increased numbers of cells in G1-phase (11%), S-phase (8%), and G2/M phases (10%) were detected in D431, S496 and E445 GSC, respectively, after BQ788 treatment (Figure 4B).

To gain further insight into the effects of the blockade of EDNRB on GSC growth, GSC were treated for 72 hrs with various doses of BQ788 or BQ123 (Figure 4C) and assayed for cell proliferation. Inhibition of proliferation was not seen when GSC (sorted or unsorted GSC) were treated with 25–100 μM BQ123, while treatment with 75 or 100 μM BQ788 reduced cell proliferation by 30 to 80% in D431, 30–60% in S496 and 40–60% in E445 (Figure 4C, a–c). The combination of BQ788 and BQ123 had no additive effect on suppressing cell growth, while a notable growth stimulation was observed in unsorted D431 and S496 by treatment with 50 μM BQ123 (Figure 4C, e). Of note, both fibroblasts and autologous glioblastoma cell lines passaged in serum-containing media that do not produce EDN3 were resistant to BQ788 treatment (Figure 4C, a–d). In contrast, both CD133+ and CD133− daughter cells sorted from sphere culture (D431 and S496) are sensitive to BQ788 treatment. BQ788 treatment also decreased clonogenic efficiency of both CD133+ and CD133− daughter cells sorted from GSC cultures that were initiated from purified CD133+ GSC (Figure 4D). Notably, untreated CD133− daughter cells are fast-growing cells, which exhibited higher clonogenic efficiency compared to those of untreated CD133+ daughter cells on day 7 after cell seeding.

In order to verify that the observed decreased proliferative activity and clonogenic efficiency caused by BQ788 is mainly due to cell apoptosis, not cell cycle arrest, the induction of GSC

apoptosis by the EDNRB antagonist was further determined using an ELISA-based cell death assay, which quantitatively detects the amount of cleaved DNA/histone complexes. Significant cell apoptosis were detected in all three GSC lines treated with 50–100 μM BQ788 when compared to untreated cells (Figure 4E). Thus, cell morphology observations, clonogenic assays, cell cycle analyses, and cell apoptosis assays suggest that EDN3/EDNRB signaling is a survival pathway for GSC.

Blockade of EDN3/EDNRB signaling leads to the loss of cell spreading/migration, self-renewal, and tumor initiation

Next, we determined whether blockade of EDN3/EDNRB signaling would weaken GSC self-renewal capability. Significant cell apoptosis and impaired GSC migration were detected in all three GSC lines treated with 50 μM BQ788 when compared to untreated cells (Figure 5A, a–f). More importantly, these BQ788-treated GSC failed to regenerate spheres when live cells were reseeded at clonal density (Figure 5A, h, j, l), indicating that the self-renewal capacity of GSC was lost. The impairment of cell migration and self-renewal by BQ788 treatment was also demonstrated in purified CD133+ GSC cells (Supplementary Figure 2). In order to study whether blocking the production of endogenous EDN3 in GSC will have impact on these GSC functions, we performed an on-target knockdown of EDN3. Treatment with EDN3 siRNA, not negative control siRNA, not only efficiently knocked down EDN3 mRNA expression (Figure 5B), but also abrogated the EDN3 peptide release (Figure 5C). More importantly, prominent cell apoptosis was only determined in GSC treated with EDN3 siRNA (Figure 5D). Microscopic changes in cellular morphology were observed, and in contrast to negative control siRNA-treated GSC (Figure 5E, c, g, k), loss of endogenous EDN3 by EDN3 siRNA treatment resulted in loss of self-renewal potential and cell migration capacity (Figure 5E, d, h, l). By contrast, GSC in negative control siRNA-treated cultures spontaneously migrated/spread out of tumor spheres and formed the surrounding monolayer (Figure 5E, q–s), implicating a role of EDN3/EDNRB signaling in GSC self-renewal and migration.

Based on the requirement of EDN3/EDNRB signaling for self-renewal, migration, and survival of GSC in culture, we test whether the EDN3/EDNRB signaling is required for maintaining the tumorigenic potential of GSC. Unsorted GSC or sorted CD133+ GSC were treated with or without 50μM BQ788 for 24 hr. The viability of the inhibitor-treated cells ranged from 80–87% was determined by trypan blue staining. Following washing, 10^4 live cells were stereotactically injected into the brains of SCID mice. Mice (15/16) which received untreated GSC developed neurological signs at weeks 14–22 post-injection. The H-E staining of tumor xenografts identified histological hallmarks of human glioblastomas (Figure 5F, a–l). In particular, the hypercellular zones surrounding necrotic foci similar to histopathological features of pseudopalisading necrosis was observed (Figure 5F, a–d). The infiltrative tumor exhibit hypercellularity, hyperchromatism, pleomorphism, mitosis, vascular endothelial hyperplasia, and oligodendroglial components were also identified (Figure 5F, e–l). On the other hand, injection of GSC pretreated with 50 μM BQ788 failed to develop a tumor (0/14) at week 25. The area of tumor injection site demonstrates no evidence of neoplastic cells (Figure 5F, m–r) and show no significant changes when compared to normal brain tissue (Figure 5F, s–v), except a scar-like feature is occasionally observed near the injection site (Fig. 5F, r). These data thus suggest the potential involvement of autocrine EDN3/EDNRB signaling in maintaining the tumorigenic capacity of GSC in culture.

To investigate whether in-vitro cultured GSC change the expression of the EDN ligands and receptors, we analyzed and compared the expression of EDN system genes in tumor xenografts (initiated from purified CD133+ GSC), and CD133+ and CD133− cells directly sorted from them, by RT-PCR (Figure 5G, a). CD133, EDN1, EDN3, and EDNRA mRNA

were determined in tumor xenografts (Figure 5G, a), whereas a lower level of EDN3 mRNA was detected compared to that of EDN1 mRNA. However, although EDNRB mRNA was detected in CD133+ GSC used for injection, it could not be detected in tumor xenografts after the 30 cycles of PCR. Similar expression patterns of the EDN system genes were also demonstrated in tumors by IHC staining (Figure 5G, b). Likewise, EDN1, EDN2, EDN3 and EDNRA mRNA were also determined in both CD133+ and CD133− cells sorted from tumor xenografts, whereas CD133+ cells express a lower level of EDN1 and a higher level of EDN3 mRNA when compared to those of CD133− cells (Figure 5G, c). YKL-40 mRNA could only be detected in tumor xenografts and sorted CD133− cells (Figure 5G, a, c). When CD133+ cells were recultured in SGF media for 7 days, the expression of EDNRB mRNA could be redetected (Figure 5G, d). On the other hand, tumor xenografts which exhibit a higher level of EDN3 mRNA and lower levels of EDN1 and EDN2 mRNA, were also identified (supplementary Figure 3). Nevertheless, a higher level of EDNRA mRNA is always expressed in tumor xenografts and sorted CD133+ and CD133− cells, whereas a low level of EDNRB mRNA could only be detected in tumor xenografts. These data may suggest that the initiation of tumor growth in vivo from GSC is accompanied with the activation/upregulation of EDNRA signaling and downregulation of EDNRB signaling.

Exogenous EDN3 alone can maintain GSC survival but not promote GSC expansion

To explore the possibility that EDN3 alone might be a growth factor or a survival factor for GSC, we removed stem cell growth factors (FGF, EGF, LIF) from the media and replaced them with various doses of recombinant EDN3. Apoptotic cells were observed in all tested GSC maintained in plain media (40–50% viable cells) and the addition of EDN3 (1–100 nM) improved the viability of GSC as determined by the trypan blue exclusion test (50–80% viability) ($p<0.05$). However, reduced viability was observed when high doses of EDN3 (300 nM and 1000 nM) were added (Figure 6A). Rescue of GSC from apoptosis by adding exogenous EDN3 was further evidenced by a quantitative apoptosis assay coupled with morphological examination (Figure 6B, 6C). In general, 30 nM EDN3 alone lowered the degree of cell apoptosis to a level close to that of SGF compared to plain media. Furthermore, low proliferative stimulation was seen with the addition of exogenous EDN3 (~1.5 fold) (Figure 6A), yet exogenous EDN3 alone was not able to propagate GSC in culture as that of SGF media, suggesting that the significance of “growth stimulation” ($p<0.05$) is likely due to significantly fewer apoptotic cells maintained when compared to cells cultured in plain media. This notion was further tested by investigating the effects of exogenous EDN3 on sorted CD133+ and CD133− daughter cells. We found that EDN3 alone could enhance the viability of both types of cells in a dose-response fashion as determined by trypan-blue staining (Figure 6D). However, in contrast to cells cultured in SGF, sphere formation and cell expansion were not achievable by EDN3 alone even when EDN3 were repetitively added daily (Supplementary Figure 4). These data therefore suggest that EDN3 alone is not a potent mitogen for GSC, but may provide cell survival benefits.

Genes regulated by EDN3/EDNRB signaling

To gain further insight into the molecular mechanisms underlying the requirement of EDN3/EDNRB signaling in maintaining GSC, we performed a large-scale gene expression comparison of GSC treated with and without EDNRB inhibitor (BQ788). Probe set signals on the expression array that were ≤ 1.5-fold lower in 3 treated (n=3 patients)versus 6 untreated GSC samples (50 μM, 24 hrs) (n=3 patients, sample duplicate) with a pairwise t-test ($P < 0.05$) were selected. Samples were permuted 100 times by dChip for a false discovery rate (FDR) of 11% (median), and 61 significant genes were obtained (Table 1). The major downregulated genes identified among 61 genes are those involved in organizing cytoskeleton structure and function (e.g. EFEMP1, IQGAP1, CADL1, WASF2, S100A6, MYO10, MYO6, CCDC88A, RHOQ, SRGAP2, PALLD, CTSB, WASL, FRMD4B, HIP1,

RAB31, VPS35), mitotic spindle assembly, mitotic checkpoint (e.g. ASPM, NUSAP1, ASPM, USAP1), and DNA repair or antiapoptosis (e.g. UHMK1, NIPBL, KRAS, G2E3, DHX9, GTSE1, RIF1, NAA15), reflecting disruptions in cell structure, cell polarity, cell movement, intracellular transports, cell division and cell survival pathway. Concomitantly, a series of genes that provides negative regulation of development, cell growth, and differentiation were identified (e.g. IFI27, SOCS3, MTUS1, SCML1, IFI16, LUZP1, IL6ST, JMJD1C, TEAD1, LINGO1, C9orf86, PSD3, USP10), suggesting the stemness properties and cellular quiescence in GSC were disturbed. The distinctive gene expression profiles of randomly selected genes were verified by qt-RT-PCR (Supplementary Figure 5). Correspondingly, GSEA identified 97 significant gene ontology (GO) clusters (Supplemental Table 1) mostly associated with microtubule cytoskeleton organization, cell division, motor activity, spindle, DNA packaging, leading edge, transcription repressor activity, negative regulation of DNA binding, detection of chemical stimulus, cell cycle arrest, and neuron development, offering a potential molecular explanation for how loss of EDN3/EDNRB signaling may impact GSC migration, self-renewal, cell survival, and tumorigenic capacity. We used the default parameters of GSEA and Gene Ontology gene sets were permuted 1000 times. We called a gene set significant if the FDR q-value was under 0.15. BQ788 works by potently and competitively inhibiting EDN3 binding to EDNRB; therefore, it may explain that downregulation of EDNRB transcripts by BQ788 treatment was not determined either by expression microarray or RT-PCR (data not shown). However, several GSC genes (e.g. EFEMP, IQGAP1, SOCS3, WAVE2, MYO10, K-RAS) down-regulated by BQ788 treatment have been previously reported to be linked to activation of mitogen-activated protein kinase (MAPK) pathways (supplemental Table 2), which are the downstream effector pathways of EDNRB signaling pathway (38–43), suggesting that the identified genes characterizing stemness, migration, and survival of GSC are regulated by EDN3/EDNRB signaling.

Discussion

The finding of EDN3 overexpression in GSC through the expression microarray analysis led to our novel investigation of the EDN system in cultured GSCs. In normal NCC cultures, EDN3/EDNRB signaling prevents the premature differentiation of crest-derived precursors (22, 44). In vivo, EDN3/EDNRB signaling is required for NCC migration during ENS development (22). Mutations in EDN3 or EDNRB can lead to the abnormal development of ENS and melanocytes, implying that the loss of function in these two genes may interfere with tumor development by EDN3/EDNRB signaling-dependent GSC. Indeed, blockade of EDN3/EDNRB signaling of GSC leads to the loss of tumorigenic potential in our GSC model. We found that cultured GSC express both neural and mesenchymal signatures characterizing NCC-like cells and therefore hypothesized that autocrine EDN3/EDNRB signaling may be a survival/maintenance factor for GSC. In fact, when GSC undergo serum-induced proliferative differentiation, a significant loss of EDN3 production accompanied by co-downregulation of a series of transcripts related to NCC, RGC and NSC was observed. For instance, SOX2 is a marker of NSC and is essential for maintaining the pluripotent, self-renewal, and undifferentiated phenotypes of embryonic stem cells. Moreover, silencing of SOX2 in GSC can cause the loss of tumorigenicity (45). FABP7, a glial-specific marker, is a direct target of Notch signaling in RGC, and the involvement of Notch signaling in the maintenance of the tumorigenic potential of GSC has been reported (46). Thus, autocrine EDN3/EDNRB signaling may prevent GSC from differentiating prematurely.

Direct evidence of the differentiation-inhibiting effect of EDN3 was demonstrated in clonogenic cultures of ENS progenitors supplemented with EDN3, by which neuronal and glial differentiation pathways were blocked and the multipotent state of progenitors was maintained (44, 47). These observations thus support the view that autocrine EDN3

maintains the undifferentiated state of GSC. Moreover, EDN3 and EDN1 mRNAs are altered reciprocally in GSC in response to differentiation, indicating that EDN3 and EDN1 genes can be epigenetically regulated, and that increased EDN1 may be associated with the onset of tumorigenesis. Indeed, we detected an increased expression of EDN1, but not EDN3, mRNA in patient glioblastoma tumors (compared to GSC), suggesting that EDN3 may play a tumor suppressor-like role to maintain the quiescence and tumorigenic potential of GSC. In agreement with this, a frequent loss of EDN3 expression in breast tumors due to epigenetic inactivation has previously been suggested (29). Likewise, there were decreased levels of EDN3 and increased levels of EDN1 and EDN2 mRNA in cancerous cervical epithelial cells compared with normal cervical epithelial cells (28). Thus, the reduction of EDN3 levels (e.g. induced by exogenous cues) may implicate the initiation of proliferative differentiation from quiescent GSC towards more differentiated progeny, by which the proliferative progeny gradually overpopulate a tumor. It appears that sole EDN3/EDNRB signaling alone cannot grant tumorigenic potential to GSC, yet the removal of EDN3/EDNRB signaling contributed undifferentiated, anti-apoptotic, and migratory properties to GSC, which may weaken or eliminate their tumorigenic capacity. Autocrine EDN3 in EDNRB+ GSC, may therefore, play a role in anti-developmental, anti-differentiating, antiapoptotic and anti-tumorigenic functions, thereby help in maintaining a continuous GSC pool.

We found that loss of EDN3 production in GSC through serum-induced differentiation did not cause cell apoptosis, while directly blocking EDN3/EDNRB signaling causes severe GSC apoptosis. These observations seem to support the notion that autocrine EDN3/EDNRB signaling only provides survival benefits when GSC are maintained in SGF condition. A previous study has shown that stimulation of the EDNRB in astrocyte induces cAMP response element-binding protein (CREB) and c-fos expression via multiple MAPK signaling pathways, including the extracellular regulated kinase (ERK) 2, c-Jun N-terminal kinase 1 (JNK1), and p38 kinase (38). EDN3 stimulation also rapidly increased phosphorylation of ERK2 in neural progenitor cells (39) and activated IkappaB and MAPK in the human colonic epithelial cells (40). Likewise, EDN3 treatment resulted in the activation of MAPK-p90 ribosomal S6 kinase-CREB and cAMP-protein kinase A-CREB pathways in melanocyte culture (41, 42) and induction of ERK1/2 and focal adhesion kinase (FAK) phosphorylation in malenoma cells (43). One important note is that the activation of EDNRB by EDN3 also leads to loss of expression of the cell adhesion molecule E-cadherin and associated catenin proteins, while increasing Snail and N-cadherin expression (43). Thus, the expression profiles of BQ788-treated GSC supports the notion that these pathways are the downstream effector pathways of EDN3/EDNRB signaling pathway that contribute GSC survival and migration (Supplementary Table 2). The usage of an inducible knockdown of EDNRB would strengthen the role of EDNRB signaling in GSC. Moreover, since ex-vivo treatment with BQ788 may already damage the capabilities of self-renewal and proliferative differentiation in GSC, inducible knockdown of EDNRB or EDN3 using viral-delivered hairpin RNA would allow more in depth functional and in vivo studies.

It has been shown that EDN3 first stimulates expression of EDNRB, then when under prolonged exposure to EDN3, EDNRB expression decreases (12). This may explain why EDNRB are expressed at lower levels in the sphere cultures, which consistently produce EDN3. We found that EDN3 alone is not a potent mitogen for GSC and similar finding was also reported (44). Interestingly, it was shown that EDNRB antagonists reduced the viability and proliferation of glioma cells, which do not express EDN3 (48), implying the possibility of blocking EDN1/EDNRB signaling. The decreased glioma cell viability by EDNRB antagonists independent of their cognate receptor was also reported (49). We speculate that low levels of EDNRB mRNA being expressed in cultured CD133+ GSC used for injection, but not in some tumor xenografts, could be due to tumor initiation from CD133+ GSC being

accompanied by activation/upregulation of EDNRA signaling and downregulation of EDNRB signaling in our model system. Alternatively, it is possible that EDNRB may be only expressed by a small subset of quiescent GSC that express the tumor-suppressive phenotype (e.g. CD133+/EDNRB+ cells) for maintaining GSC pool in vivo, which can be retrieved and enriched by SGF culturing. On the other hand, CD133+ cells sorted from xenografts may mostly contain activated GSC (e.g. CD133+/EDNRB-/EDNRA+ cells) that have entered the pathway to tumorigenesis. Interestingly, some tumor xenografts express high levels of EDN3 and EDNRA mRNA, but low levels of EDN1 and EDN2 mRNA, with a negligible level of EDNRB mRNA, suggesting that the growth of EDN3+ tumor may not be EDNRB, but EDNRA signaling-dependent. Promoter hypermethylation of the EDNRB gene in various human malignancies has been reported and suggested that EDNRB may be a candidate tumor-suppressor gene (50).

Lastly, our genome-wide expression analysis has provided some molecular explanation for the requirement of EDN3/EDNRB signaling in maintaining GSC sphere cultures. Apparently, EDN3/EDNRB blockade mostly impacts cell structure, cell movement, self-renewal/cell division, and cell survival, rendering GSC non-tumorigenic. We previously demonstrated that CD133+ cells, not CD133− cells, sorted from same sphere cultures contain enriched tumorigenic cells yet they express tumor suppressor phenotype (8). Thus, true GSC may be quiescent prior to undergoing asymmetric cell division to simultaneously self-renew and generate more differentiated progeny. It appears that differentiated progeny are active-growing cells that make up the most population in tumor spheres and are likely the effector progeny which can undergo proliferative differentiation to produce more differentiated progeny that expresses hyperproliferative and hyperangiogenic phenotype, leading to tumor formation in animals. Therefore, identifying essential genes (e.g. EDN3) which are shared by both GSC and their immediate differentiated progeny/daughter cells would enhance its clinical value since both populations can be targeted. Thus, treatment with BQ788 not only abolishes the self-renewal capacity of quiescent GSC but also prevent differentiated progeny from populating tumor spheres and forming tumor in animals.

Depletion of EDN3+ cells will likely prevent either CD133+ or CD133− GSC from regenerating a tumor. Futures studies should determine whether addition of EDNRB antagonist can sensitize cells to radio-chemotherapy in treatment of established glioblastoma tumors in animals. Our data support the view that the prevention of GSC-mediated tumor recurrence may need to focus on targeting active stem cell pathways in GSC (such as EDN3/EDNRB pathway), not proliferative pathways. Obviously, the cure for brain cancer requires eliminating both GSC and non-GSC populations; therefore, it is important to evaluate the synergistic benefits of incorporating GSC-targeted therapies into conventional cancer treatments.

Supplementary Material

Refer to Web version on PubMed Central for supplementary material.

Acknowledgments

Grant support

This work was supported by grants from the American Cancer Society (RSG-07-109-01-CCE), National Cancer Institute (1 R21 CA140912-01), National Institute of Health (1DP2OD006444-01), and The Bradley Zankel Foundation to C-L T.

References

1. Maher EA, Furnari FB, Bachoo RM, et al. Malignant glioma: genetics and biology of a grave matter. Genes Dev. 2001; 15:1311–1333. [PubMed: 11390353]
2. Beier D, Hau P, Proescholdt M, et al. CD133(+) and CD133(−) glioblastoma-derived cancer stem cells show differential growth characteristics and molecular profiles. Cancer Res. 2007; 67:4010–4015. [PubMed: 17483311]
3. Gunther HS, Schmidt NO, Phillips HS, et al. Glioblastoma-derived stem cell-enriched cultures form distinct subgroups according to molecular and phenotypic criteria. Oncogene. 2008; 27:2897–2909. [PubMed: 18037961]
4. Hemmati HD, Nakano I, Lazareff JA, et al. Cancerous stem cells can arise from pediatric brain tumors. Proc Natl Acad Sci USA. 2003; 100:15178–15183. [PubMed: 14645703]
5. Singh K, Hawkins C, Clarke ID, et al. Identification of human brain tumour initiating cells. Nature. 2004; 432:396–401. [PubMed: 15549107]
6. Wang J, Sakariassen PO, Tsinkalovsky O, et al. CD133 negative glioma cells form tumors in nude rats and give rise to CD133 positive cells. Int J Cancer. 2008; 122:761–768. [PubMed: 17955491]
7. Galli R, Binda E, Orfanelli U, et al. Isolation and characterization of tumorigenic, stem-like neural precursors from human glioblastoma. Cancer Res. 2004; 64:7011–7021. [PubMed: 15466194]
8. Liu Q, Nguyen DH, Dong Q, et al. Molecular properties of CD133+ glioblastoma stem cells derived from treatment-refractory recurrent brain tumors. J Neurooncol. 2009; 94:1–19. [PubMed: 19468690]
9. Yuan X, Curtin J, Xiong Y, et al. Isolation of cancer stem cells from adult glioblastoma multiforme. Oncogene. 2004; 23:9392–9400. [PubMed: 15558011]
10. Bao S, Wu Q, McLendon RE, et al. Glioma stem cells promote radioresistance by preferential activation of the DNA damage response. Nature. 2006; 444:756–760. [PubMed: 17051156]
11. Murat A, Migliavacca E, Gorlia T, et al. Stem cell-related “self-renewal” signature and high epidermal growth factor receptor expression associated with resistance to concomitant chemoradiotherapy in glioblastoma. J Clin Oncol. 2008; 26:3015–3024. [PubMed: 18565887]
12. Lahav R, Dupin E, Lecoin L, et al. Endothelin 3 selectively promotes survival and proliferation of neural crest-derived glial and melanocytic precursors in vitro. Proc Natl Acad Sci USA. 1998; 95:14214–14219. [PubMed: 9826680]
13. Stone JG, Spirling LI, Richardson MK. The neural crest population responding to endothelin-3 in vitro includes multipotent cells. J Cell Sci. 1997; 110 (Pt 14):1673–1682. [PubMed: 9247201]
14. Rubanyi GM, Polokoff MA. Endothelins: molecular biology, biochemistry, pharmacology, physiology, and pathophysiology. Pharmacol Rev. 1994; 46:325–415. [PubMed: 7831383]
15. Shimada K, Matsushita Y, Wakabayashi K, et al. Cloning and functional expression of human endothelin-converting enzyme cDNA. Biochem Biophys Res Commun. 1995; 207:807–812. [PubMed: 7864876]
16. Bagnato A, Catt KJ. Endothelins as autocrine regulators of tumor cell growth. Trends Endocrinol Metab. 1998; 9:378–383. [PubMed: 18406309]
17. Leibl MA, Ota T, Woodward MN, et al. Expression of endothelin 3 by mesenchymal cells of embryonic mouse caecum. Gut. 1999; 44:246–252. [PubMed: 9895385]
18. Levin ER. Endothelins. N Engl J Med. 1995; 333:356–363. [PubMed: 7609754]
19. Edery P, Attie T, Amiel J, et al. Mutation of the endothelin-3 gene in the Waardenburg-Hirschsprung disease (Shah-Waardenburg syndrome). Nat Genet. 1996; 12:442–444. [PubMed: 8630502]
20. McCallion AS, Chakravarti A. EDNRB/EDN3 and Hirschsprung disease type II. Pigment Cell Res. 2001; 14:161–169. [PubMed: 11434563]
21. Brand M, Le Moullec JM, Corvol P, Gasc JM. Ontogeny of endothelins-1 and -3, their receptors, and endothelin converting enzyme-1 in the early human embryo. J Clin Invest. 1998; 101:549–559. [PubMed: 9449687]
22. Nagy N, Goldstein AM. Endothelin-3 regulates neural crest cell proliferation and differentiation in the hindgut enteric nervous system. Dev Biol. 2006; 293:203–217. [PubMed: 16519884]

23. Egidy G, Eberl LP, Valdenaire O, et al. The endothelin system in human glioblastoma. Lab Invest. 2000; 80:1681–1689. [PubMed: 11092528]
24. Tsutsumi K, Niwa M, Kitagawa N, et al. Enhanced expression of an endothelin ETA receptor in capillaries from human glioblastoma: a quantitative receptor autoradiographic analysis using a radioluminographic imaging plate system. J Neurochem. 1994; 63:2240–2247. [PubMed: 7964744]
25. Bhalla A, Haque S, Taylor I, Winslet M, Loizidou M. Endothelin receptor antagonism and cancer. Eur J Clin Invest. 2009; 39(Suppl 2):74–77. [PubMed: 19335749]
26. Subramanian A, Tamayo P, Mootha, et al. Gene set enrichment analysis: a knowledge-based approach for interpreting genome-wide expression profiles. Proc Natl Acad Sci U S A. 2005; 102:15545–50. [PubMed: 16199517]
27. Lee J, Kotliarova S, Kotliarov Y, et al. Tumor stem cells derived from glioblastomas cultured in bFGF and EGF more closely mirror the phenotype and genotype of primary tumors than do serum-cultured cell lines. Cancer Cell. 2006; 9:391–403. [PubMed: 16697959]
28. Sun de J, Liu Y, Lu DC, et al. Endothelin-3 growth factor levels decreased in cervical cancer compared with normal cervical epithelial cells. Hum Pathol. 2007; 38:1047–1056. [PubMed: 17445867]
29. Wiesmann F, Veeck J, Galm O, et al. Frequent loss of endothelin-3 (EDN3) expression due to epigenetic inactivation in human breast cancer. Breast Cancer Res. 2009; 11:R34. [PubMed: 19527488]
30. Kurtz A, Zimmer A, Schnutgen F, et al. The expression pattern of a novel gene encoding brain-fatty acid binding protein correlates with neuronal and glial cell development. Development. 1994; 120:2637–2649. [PubMed: 7956838]
31. Uchida N, Buck DW, He D, et al. Direct isolation of human central nervous system stem cells. Proc Natl Acad Sci USA. 2000; 97:14720–14725. [PubMed: 11121071]
32. Ellis P, Fagan BM, Magness ST, et al. SOX2, a persistent marker for multipotential neural stem cells derived from embryonic stem cells, the embryo or the adult. Dev Neurosci. 2004; 26:148–165. [PubMed: 15711057]
33. Yun K, Mantani A, Garel S, Rubenstein J, Israel MA. Id4 regulates neural progenitor proliferation and differentiation in vivo. Development. 2004; 131:5441–5448. [PubMed: 15469968]
34. Shen Y, Mani S, Meiri KF. Failure to express GAP-43 leads to disruption of a multipotent precursor and inhibits astrocyte differentiation. Mol Cell Neurosci. 2004; 26:390–405. [PubMed: 15234344]
35. Pelloski CE, Mahajan A, Maor M, et al. YKL-40 expression is associated with poorer response to radiation and shorter overall survival in glioblastoma. Clin Cancer Res. 2005; 11:3326–3334. [PubMed: 15867231]
36. Mitaka C, Hirata Y, Ichikawa K, et al. Effects of TNF-alpha on hemodynamic changes and circulating endothelium-derived vasoactive factors in dogs. Am J Physiol. 1994; 267:H1530–1536. [PubMed: 7943398]
37. Thomson E, Kumarathasan P, Vincent R. Pulmonary expression of preproET-1 and preproET-3 mRNAs is altered reciprocally in rats after inhalation of air pollutants. Exp Biol Med (Maywood). 2006; 231:979–984. [PubMed: 16741034]
38. Schinelli S, Zanassi P, Paolillo M, et al. Stimulation of endothelin B receptors in astrocytes induces cAMP response element-binding protein phosphorylation and c-fos expression via multiple mitogen-activated protein kinase signaling pathways. J neurosci. 2001; 21:8842–8853. [PubMed: 11698596]
39. Shinohara H, Udagawa J, Morishita R, et al. Gi2 signaling enhances proliferation of neural progenitor cells in the developing brain. J Biol Chem. 2004; 279:41141–41148. [PubMed: 15272018]
40. Kalabis J, Li G, Fukunaga-Kalabis M, Rustgi AK, Herlyn M. Endothelin-3 stimulates survival of goblet cells in organotypic cultures of fetal human colonic epithelium. Am J Physiol Gastrointest Liver Physiol. 2008; 295:G1182–1189. [PubMed: 18832450]
41. Bohm M, Moellmann G, Cheng E, et al. Identification of p90RSK as the probable CREB-Ser133 kinase in human melanocytes. Cell Growth Differ. 1995; 6:291–302. [PubMed: 7540859]

42. Sato-Jin K, Nishimura EK, Akasaka E, et al. Epistatic connections between microphthalmia-associated transcription factor and endothelin signaling in Waardenburg syndrome and other pigmentary disorders. FASEB J. 2008; 22:1155–1168. [PubMed: 18039926]
43. Bagnato A, Rosano L, Spinella F, et al. Endothelin B receptor blockade inhibits dynamics of cell interactions and communications in melanoma cell progression. Cancer Res. 2004; 64:1436–1443. [PubMed: 14973117]
44. Wu JJ, Chen JX, Rothman TP, Gershon MD. Inhibition of in vitro enteric neuronal development by endothelin-3: mediation by endothelin B receptors. Development. 1999; 126:1161–1173. [PubMed: 10021336]
45. Gangemi RM, Griffero F, Marubbi D, et al. SOX2 silencing in glioblastoma tumor-initiating cells causes stop of proliferation and loss of tumorigenicity. Stem Cells. 2009; 27:40–48. [PubMed: 18948646]
46. Fan X, Khaki L, Zhu TS, et al. NOTCH pathway blockade depletes CD133-positive glioblastoma cells and inhibits growth of tumor neurospheres and xenografts. Stem Cells. 2010; 28:5–16. [PubMed: 19904829]
47. Bondurand N, Natarajan D, Barlow A, Thapar N, Pachnis V. Maintenance of mammalian enteric nervous system progenitors by SOX10 and endothelin 3 signalling. Development. 2006; 133:2075–2086. [PubMed: 16624853]
48. Paolillo M, Russo MA, Curti D, et al. Endothelin B receptor antagonists block proliferation and induce apoptosis in glioma cells. Pharmacol Res. 2010; 61:306–315. [PubMed: 19931393]
49. Montgomery JP, Patterson PH. Endothelin receptor B antagonists decrease glioma cell viability independently of their cognate receptor. BMC Cancer. 2008; 8:354–364. [PubMed: 19040731]
50. Pao MM, Tsutsumi M, Liang G, et al. The endothelin receptor B (EDNRB) promoter displays heterogeneous, site specific methylation patterns in normal and tumor cells. Hum Mol Genet. 200; 10:903–910. [PubMed: 11309363]

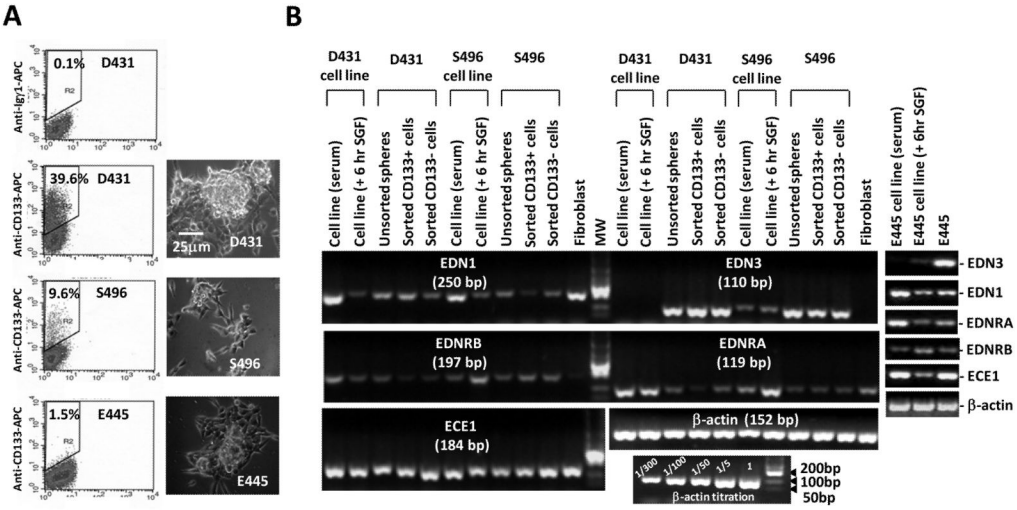

Figure 1.

Presence of endothelin system components in GSC. A. Tumorigenic GSC cultures, D431, S496 and E445, were established from patient-derived glioblastoma tumors. Percentages of CD133+ cells in each culture were determined by flow cytometry analysis using anti-CD133 directly conjugated to allophycocyanin (APC). GSC cultures form semi-adherent tumor spheres with cells spontaneously migrating out of spheres. Scale bar = 25 μm. B. Total RNA from the indicated GSC cultured in SGF media, autologous glioblastoma cell lines cultured in serum-containing media and switched to SGF media for 6 h, and fibroblasts cultured in serum-containing media were extracted. The mRNA expression levels of EDN-1, EDN-3, EDNRA, EDNRB, and ECE-1 were analyzed by qtRT-PCR with specific primers. β-actin was used as an internal control gene.

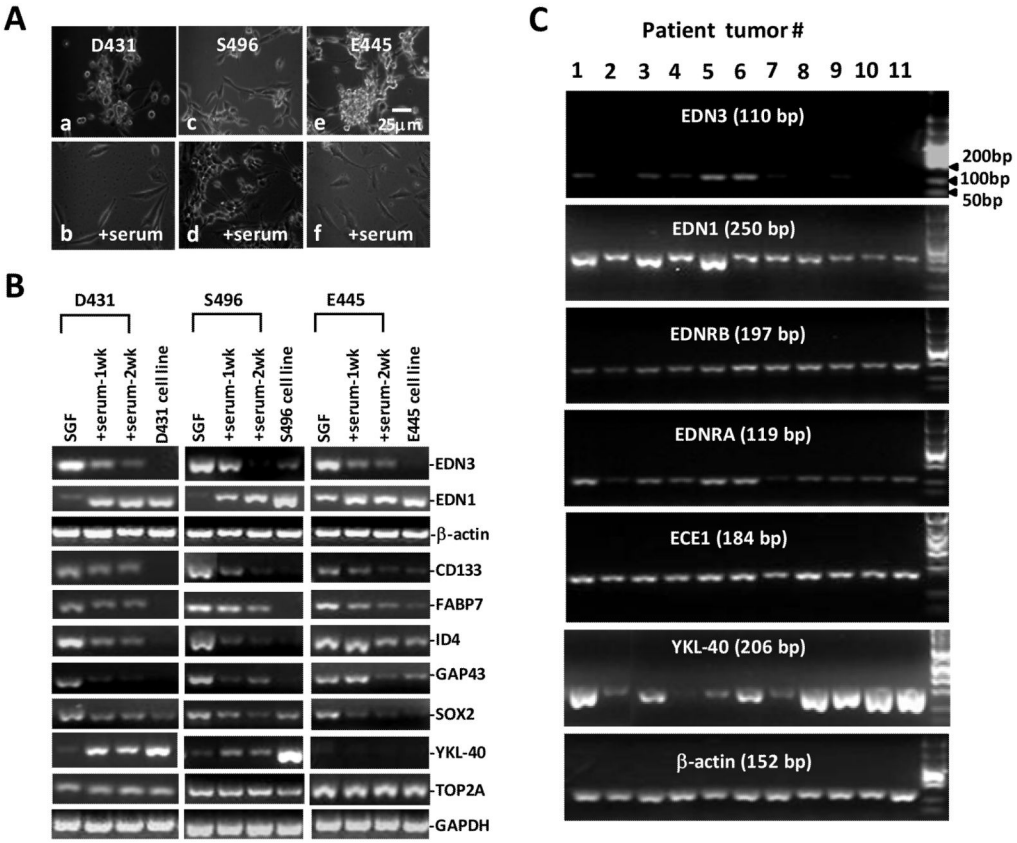

Figure 2.

Reciprocal regulation and expression of EDN1 and EDN3 mRNA in GSC and glioblastoma tumors. A. Light-microscopic morphology of indicated GSC cultures before (a, c, e) and after two-week serum-induced proliferative differentiation (b, d, f). Scale bar = 25 μm. B. The indicated GSC cultures were switched to serum-containing media for the time shown. The mRNA expression levels of EDN1 and EDN3 and the indicated NSC (CD133, SOX2, ID4), RGC (FABP7), and glioblastoma-associated genes (YKL-40, TOP2A) were analyzed by qtRT-PCR with specific primers. β-actin and GAPDH were used as internal control genes. C. Total RNA from patient-derived glioblastoma tumors (n=11) were extracted. The mRNA expression levels of the indicated endothelin system components were analyzed by qtRT-PCR with specific primers. YKL-40 represents a glioblastoma progression-associated gene, and β-actin was used as an internal control gene.

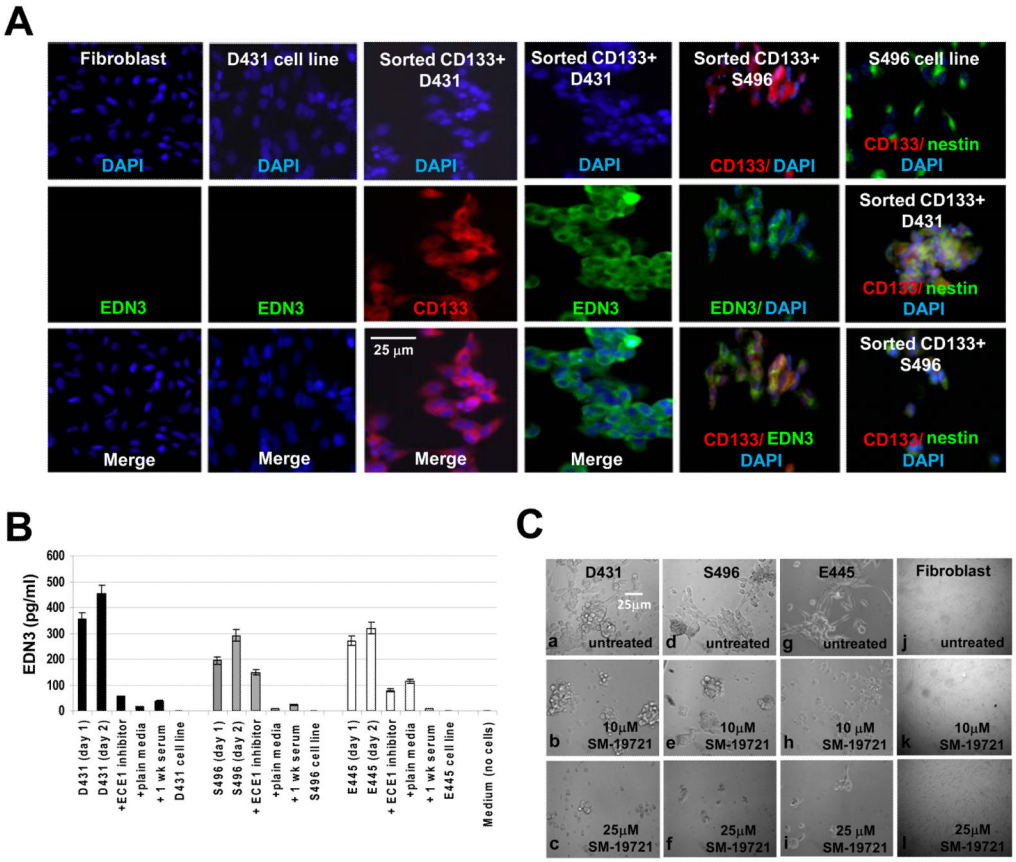

Figure 3.

GSC express and secret EDN3. A. The indicated GSC lines and autologous glioblastoma cell lines were subjected to single or dual color-fluorescent immunocytochemical analysis for the expression of EDN3, CD133 and nestin. The fluorescent stain DAPI was used to counterstain nuclei. Scale bar = 25μm. B. The amounts of EDN3 protein peptides secreted into the conditioned media by GSC (5×10^4 cells/ml/well) cultured under the indicated conditions were determined by an anti-EDN3 quantitative ELISA kit and were presented as picograms per milliliter (pg/ml). The indicated glioblastoma cell lines were cultured in serum-containing media. Data represent mean values ± SD of triplicate measurements in triplicate experiments. C. Light-microscopic morphology of GSC cultures and fibroblasts (5×10^4 cells/ml/well) treated with and without ECE-1 inhibitor (SM-1972) at the indicated concentrations for 7 days. Scale bar = 25μm.

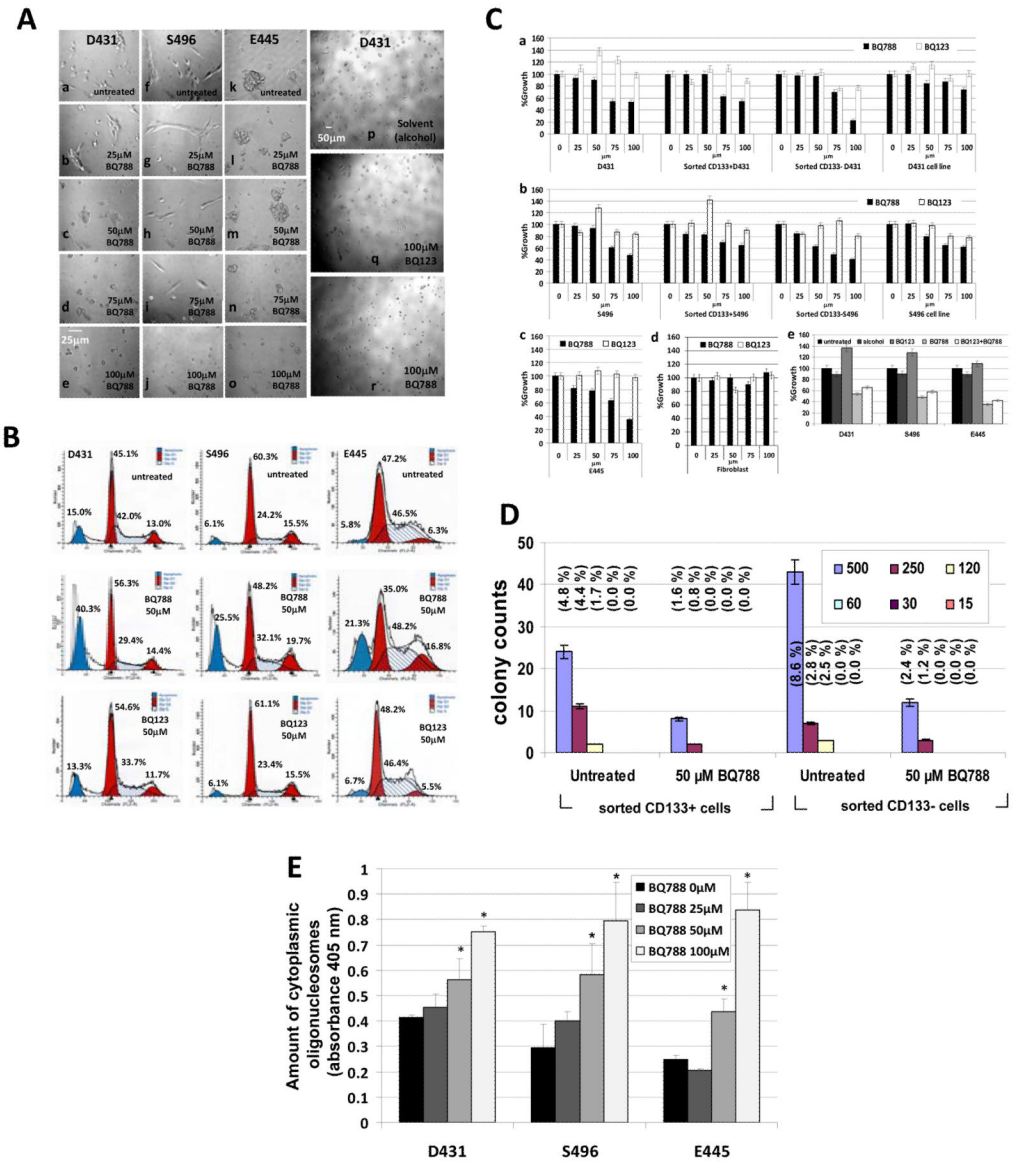

Figure 4.

Blockade of EDNRB not EDNRA induces GSC apoptosis independent from cell-cycle arrest. A. Light-microscopic morphology of GSC cultures treated with the indicated concentrations of BQ788, BQ123, or vehicle control (ethanol alcohol) for 3 days. Scale bar = 25 μm or 50 μm. B. The indicated GSC lines were treated with 50 μM BQ788 or BQ123 for 3 days, and cell cycle distributions including sub-G1 fraction were determined by flow cytometric analysis. C. The sorted CD133+ and CD133− cells and unsorted GSC lines, autologous glioblastoma cell lines, and fibroblasts were treated with BQ788, BQ123 (a–d), or combinations (e) at the indicated concentrations for three days. The cell growth was determined by MTS/PMS cell proliferation assays. Data represent mean values ± SD of triplicate measurements in triplicate experiments. D. CD133+ and CD133− daughter cells sorted from sphere cultures that initiated from purified CD133+ GSC were seeded at the indicated cell density per well in 96-well plate by limiting dilution in 100 μl SGF media. The clonogenic efficiency was determined under the presence or absence of 50μM BQ788 treatment. Colonies containing more than 20 cells were counted at day 7 after cell seeding.

Data represent mean values ± SD of triplicate measurements in triplicate experiments. % clonogenic efficiency was indicated. E. The indicated GSC cultures were treated with BQ788 at the indicated concentrations for 3 days, and cell apoptosis were determined by a Cell Death Detection ELISAPLUS kit, which quantitatively detects the amount of cytoplasmic oligonucleosomes. Data represent mean values ± SD of triplicate measurements in triplicate experiments. *$p < 0.05$ versus untreated cells.

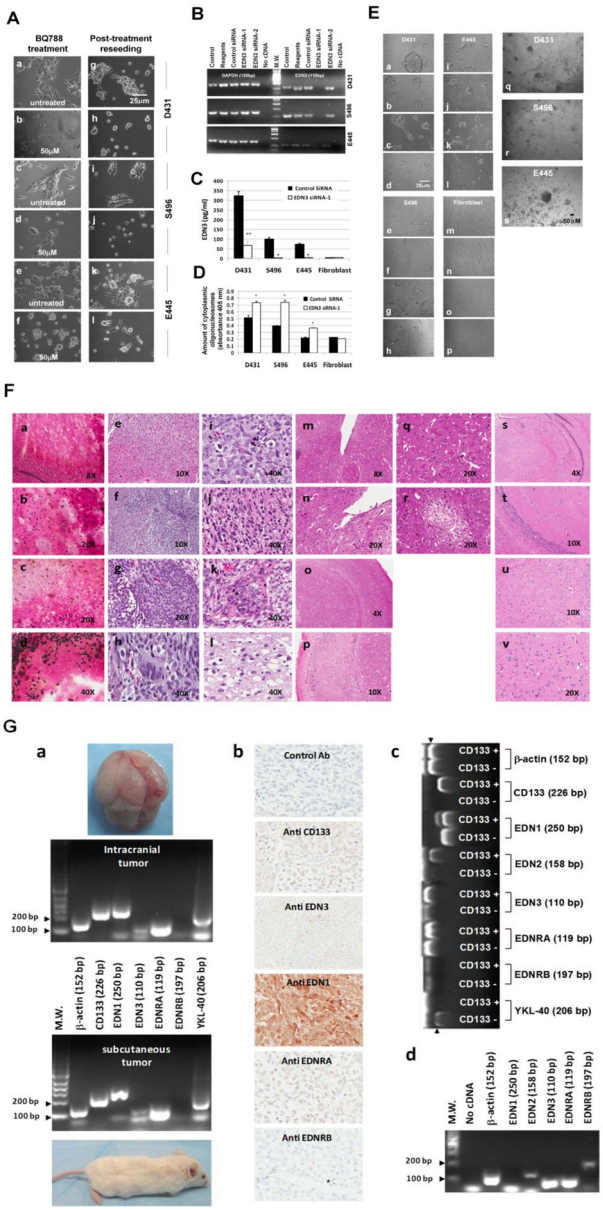

Figure 5.

Blockade of EDN3/EDNRB signaling impairs GSC self-renewal, cell migration, and tumorigenic capacity. A. Light-microscopic morphology of GSC cultures. The indicated GSC cultures were treated with and without BQ788 at the concentration of 50 μM for three days and the pictures were taken (a–f). Cells were harvested and were reseed at clonal density, which prevent cells from forming aggregates. The cultures were incubated for three days and pictures were taken (g–l). Scale bar = 25 μm. B. The indicated GSC cultures were transfected with negative control siRNA, EDN3 siRNA (clone #1 and clone#2), or treated with or without transfection reagents. Cells were incubated for 3 days and the levels of EDN3 mRNA were assayed by qtRT-PCR. The GAPDH was used as an internal control gene. Fibroblasts serve as a negative control cell line, which does not express EDN3 (data not shown). C. EDN3 protein peptides concentrations secreted into the conditioned media by transfected cells were assayed by anti EDN3 ELISA kit. Data represent mean values ± SD of triplicate measurements in triplicate experiments. *$p < 0.05$, **$p < 0.001$ versus control

siRNA transfected cells. D. Cell apoptosis in negative control siRNA or EDN3 siRNA transfected cells was determined by a cell death detection ELISA kit. Data represent mean values ± SD of triplicate measurements in triplicate experiments. *$p < 0.05$ versus control siRNA-treated cells. E. Light-microscopic morphology of indicated cells treated with assay buffer (a, e, i, m), transfection reagents (b, f, j, n), negative control siRNA (c, g, k, o), and EDN3 siRNA-1 (d, h, l, p) for 72 hrs, as well as negative control siRNA for 7 day (q–s). Scale bar = 25μm or 50μm. F. Representative photographs of hematoxylin and eosin (HE) staining of mouse brain tissue. Brain tissues from mice injected with untreated GSC display invasive growth of gliomas with diffuse infiltration into the surrounding tissue and vessels (a-l). Infiltrating tumor exhibits hypercellular zones surrounding necrotic foci and forms a ‘pseudo-palisading’ necrosis pattern (S496, frozen section) (a–d). Other important histopathological features of glioblastoma are also seen in tumor lesions, including hypercellularity (e), hyperchromatism (f, g), pleomorphism and mitosis (h–j), vascular endothelial hyperplasia (k), and oligodendroglial component (l) (D431, S496, E445). Mouse brains injected with GSC pretreated with 50μM BQ788 showed no evidence of tumor development (m–r). Mouse brain injected with stem cell media serves as control for normal brain tissue (s–u). Magnification, 4X (o, s), 8X (a, m), 100X (e, f, p, t, u), 200X (b, c, g, n, q, r, v), 400X (d, h–l). G. Presence of endothelin system components in glioma xenografts. The expression of the indicated endothelin system components in both subcutaneous and intracranial glioma xenografts were analyzed by qtRT-PCR with specific primers. β-actin was used as an internal control gene (a). Representative immunohistochemical stainings of endothelin components in intracranial tumor exnografts (b). The mRNA levels of the endothelin system components in uncultured CD133+ and CD133− cells directly sorted from the glioma xenografts were analyzed by qtRT-PCR (c). The expressions of endothelin system transcripts in CD133+ cells re-cultured in SGF media for 7 days (d).

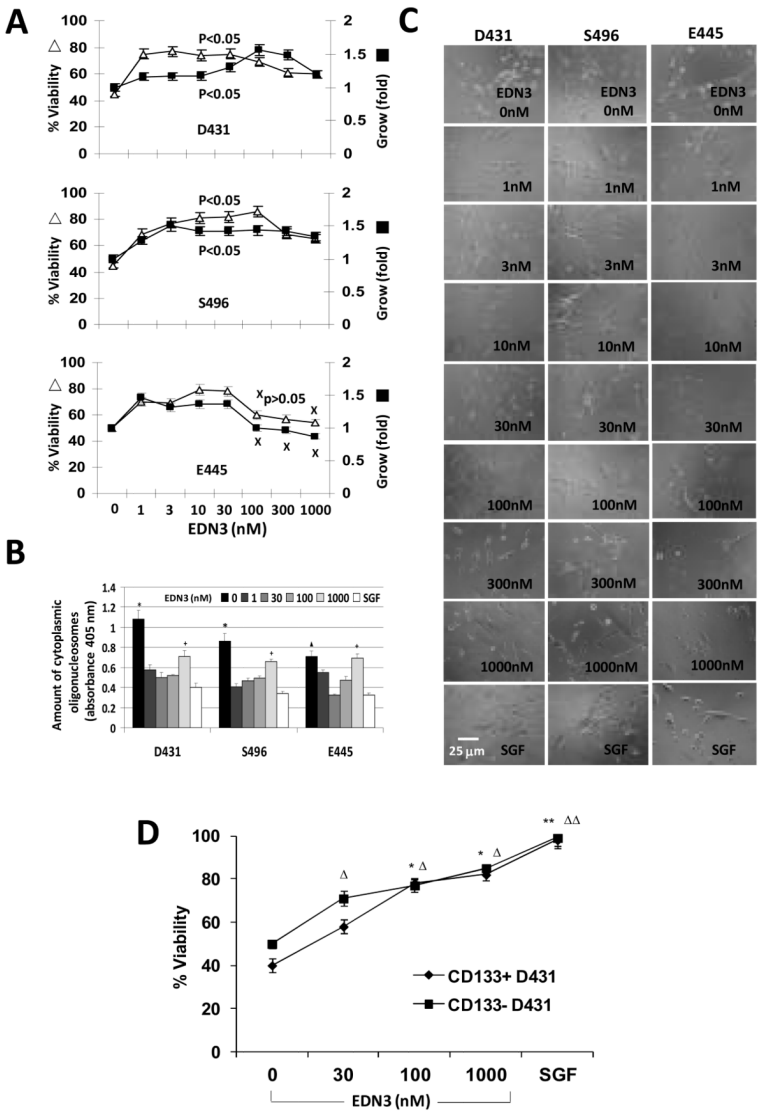

Figure 6. EDN3 is a survival factor for GSC

A. The indicated GSC lines were cultured in the plain media supplemented with various doses of EDN3 as indicated. Cells were incubated for three days and viability was determined by manually counting the trypan blue-stained samples in a hemacytometer chamber and present as percentage of viable cells in cultures (△). The cell growth was determined by MTS/PMS cell proliferation assays and present as fold increase compared to non-treated cells (■). Data represent mean values ± SD of triplicate measurements in triplicate experiments. ^{X}P>0.05 versus cells cultured in plain media. B. Cell apoptosis in (A) was assayed by a cell death detection ELISA kit. Data represent mean values ± SD of triplicate measurements in triplicate experiments. *p<0.05 versus D431 and S496 GSC treated with 1, 30, 100, 1000 nM EDN3 and SGF media. ▲p<0.05 versus E445 cells treated with 1, 30, 100 nM EDN-3 and SGF media. +P<0.05 versus D431, S496, and E445 cultured in SGF media. C. Light-microscopic morphology of cell cultures in (A). Scale bar = 25 µm. D. Cell survival was assayed in sorted CD133+ and CD133− GSC cells cultured in the SGF, plain media or plain media supplemented with various doses of EDN3 as indicated. Cells were incubated for 7 days and viability was determined by trypan blue staining. Data represent mean values ± SD of triplicate measurements in triplicate experiments. * p<0.05,

**p<0.01 (CD133+ cells), Δ p<0.05, ΔΔ p<0.01 (CD133-cells) versus cells cultured in plain media.

Table 1

Genes expressed at lower levels in BQ788 treated glioblastoma stem cells (GSC) compared with untreated GSC*

Geneff	Gene ID	Symbo l	Fold change	P value	Functional involvement
interferon, alpha-inducible protein 27	3429	IFI27	4.30	0.029619	anti-growth, anti differentiation, apoptosis
heparan sulfate (glucosamine) 3-O-sulfotransferase 1	9957	HS3ST1	4.00	0.003801	synthesis of anticoagulant heparin, anti-tumor
EGF-containing fibulin-like extracellular matrix protein 1	2202	EFEMP1	2.89	0.040817	cell adhesion and migration
asp (abnormal spindle)-like, microcephaly associated	259266	ASPM	2.61	0.004877	mitotic spindle regulation
IQ motif containing GTPase activating protein 1	8826	IQGAP1	2.45	0.000015	modulation of cell architecture
suppressor of cytokine signaling 3	9021	SOCS3	2.44	0.000182	negative regulators of cytokine signaling, tumor suppressor
caldesmon 1	800	CALD1	2.41	0.038236	smooth muscle and nonmuscle contraction
mitochondrial tumor suppressor 1	57509	MTUS1	2.36	0.002229	tumor suppressor and antimitosis
sex comb on midleg-like 1 (Drosophila)	6322	SCML1	2.28	0.000178	control of embryonic development
mex-3 homolog A	92312	MEX3A	2.26	0.002964	involvement in post-transcriptional regulatory mechanisms
interferon, gamma-inducible protein 16	3428	IFI16	2.25	0.008661	anti-growth, cellular quiescence, apoptosis
WAS protein family, member 2	10163	WASF2	2.22	0.005534	cell shape and motility
topoisomerase (DNA) I	7150	TOP1	2.20	0.002516	altering the topologic states of DNA during transcription
U2AF homology motif (UHM) kinase 1	127933	UHMK1	2.20	0.002059	prevent senescence in G0/G1; cell migration
S100 calcium binding protein A6 (calcyclin)	6277	S100A6	2.19	0.032921	cell migration/motility, antisenescence
Nipped-B homolog (Drosophila)	25836	NIPBL	2.17	0.000182	tissue development, sister chromatid cohesion, DNA repair
synaptotagmin I	6857	SYT1	2.16	0.026320	vesicular trafficking and exocytosis
myosin X	4651	MYO10	2.16	0.012113	filopodia formation
myosin VI	4646	MYO6	2.15	0.002580	intracellular vesicle and organelle transport
low density lipoprotein receptor	3949	LDLR	2.14	0.012743	cholesterol synthesis
CCDC88A coiled-coil domain containing 88A	55704	CCDC88A	2.12	0.006578	actin organization, cell motility/migration
leucine zipper protein 1	7798	LUZP1	2.12	0.015862	embryonic development of brain
v-Ki-ras2 Kirsten rat sarcoma viral oncogene homolog	3845	KRAS	2.10	0.001864	possessing intrinsic GTPase activity, antiapoptosis
ectodermal-neural cortex (with BTB-like domain)	8507	ENC1	2.06	0.020856	actin-binding protein; oxidative stress response
RNA binding motif protein 8A	9939	RBM8A	2.06	0.004386	coupling pre- and post-mRNA splicing events
DEP domain containing 1	55635	DEPDC1	2.05	0.007013	cancer/testis antigen
G2E3 G2/M-phase specific E3 ubiquitin protein ligase	55632	G2E3	2.04	0.004153	prevention of apoptosis in early embryogenesis
ADP-ribosylation factor-like 7	10123	ARL4C	2.02	0.022123	cholesterol transport
secretory carrier membrane protein 1	9522	SCAMP1	2.02	0.011002	carriers to cell surface in post-golgi recycling pathways

Geneff	Gene ID	Symbo l	Fold change	P value	Functional involvement
formin-like 2	114793	FMNL2	1.99	0.002077	morphogenesis, cytokinesis, and cell polarity
ras homolog gene family, member Q	23433	RHOQ	1.96	0.005201	myofibril assembly, exocytic vesicle fusion, glucose uptake
interleukin 6 signal transducer (gp130)	3572	IL6ST	1.94	0.011686	embryonic development
DEAH (Asp-Glu-Ala-His) box polypeptide 9	1660	DHX9	1.93	0.006616	DNA repair, genome stability
oxysterol binding protein-like 8	114882	OSBPL8	1.93	0.001205	intracellular lipid receptors
THO complex 2	57187	THOC2	1.92	0.000834	binds to spliced mRNAs to facilitate mRNA export
zinc finger protein 533	151126	ZNF385B	1.92	0.009225	neuronal function; RNA maturation and stability
G-2 and S-phase expressed 1	51512	GTSE1	1.91	0.007537	antiapoptosis, control DNA damage
nucleolar and spindle associated protein 1	51203	NUSAP1	1.90	0.001876	spindle microtubule organization
jumonji domain containing 1C	221037	JMJD1C	1.90	0.001287	reactivation of silenced genes in undifferentiated ES cells
TEA domain family member 1	7003	TEAD1	1.88	0.001749	transcriptional repressor; antidifferentiation
SLIT-ROBO Rho GTPase activating protein 2	23380	SRGAP2	1.87	0.000640	controlling cell spreading and cell migration
adaptor-related protein complex 1, sigma 2 subunit	8905	AP1S2	1.86	0.009349	recognition of sorting signals
palladin	23022	PALLD	1.85	0.003542	control of cell shape, adhesion, and contraction
leucine rich repeat neuronal 6A	84894	LINGO1	1.85	0.002910	negative regulator of oligodentrocyte differentiation
cathepsin B	1508	CTSB	1.82	0.007249	invasion, migration
Wiskott-Aldrich syndrome-like	8976	WASL	1.81	0.009275	induces actin polymerization and redistribution
chromosome 9 open reading frame 86	55684	C9orf86	1.81	0.001019	cell growth regulation
HIV TAT specific factor 1	27336	HTATSF1	1.79	0.007012	process of transcriptional elongation
pleckstrin and Sec7 domain containing 3	23362	PSD3	1.79	0.003251	tumor suppressor
FERM domain containing 4B	23150	FRMD4B	1.79	0.004509	cytoskeletal signals and membrane dynamics
RAP1 interacting factor homolog (yeast)	55183	RIF1	1.76	0.006310	DNA repair
discoidin, CUB and LCCL domain containing 1	285761	DCBLD1	1.76	0.011326	integral to membrane, cell adhesion
glutamyl-prolyl-tRNA synthetase	2058	EPRS	1.75	0.000371	catalyzes the aminoacylation
male sterility domain containing 2	84188	FAR1	1.74	0.005190	controls ether glycerophospholipid synthesis
huntingtin interacting protein 1	3092	HIP1	1.70	0.002967	membrane-cytoskeletal integrity
NMDA receptor regulated 1	80155	NAA15	1.68	0.003107	N-acetyltransferase, antiapoptosis
ubiquitin specific peptidase 10	9100	USP10	1.62	0.001657	cleaves ubiquitin, a regulator of p53, antitumor
Coiled-coil domain containing 75	253635	CCDC75	1.62	0.000894	unknown
RAB31, member RAS oncogene family	11031	RAB31	1.62	0.001205	vesicle and granule targeting
hepatitis B virus × associated protein	51773	RSF1	1.57	0.002448	chromatin remodeling

Geneff	Gene ID	Symbo l	Fold change	P value	Functional involvement
vacuolar protein sorting 35 (yeast)	55737	VPS35	1.54	0.000354	subunit of the retromer, vesicle transport

* Probe set signals on the expression array that were ≤ 1.5-fold lower in BQ788 treated (n=3 patients) versus untreated GSC samples (n=3 patients, sample duplicate) with a pairwise t-test ($P < 0.05$) were selected. Samples were permutated 100 times by dChip and 61 genes with median FDR=11% were obtained